Environ. Sci. Technol. **2007**, *41,* 4221–4226

Lateral and Longitudinal Variation of Hyporheic Exchange in a Piedmont Stream Pool

ROBERT J. RYAN AND
MICHEL C. BOUFADEL*

Department of Civil and Environmental Engineering, Temple University, 1947 North 12th Street, Philadelphia, Pennsylvania 19122

A conservative solute tracer experiment was conducted in Indian Creek, a small urban stream in Philadelphia, PA, to investigate the role of subsurface properties on the exchange between streamwater and the hyporheic zone (subsurface surrounding the stream). Sodium bromide (NaBr) was used as a conservative tracer, and it was monitored in the surface water and in the bed sediments of a 15 m long pool. Subsurface sampling occurred at 12 locations in the upper layer sediments (extending from 7.5 to 10 cm below the streambed) and 13 locations in the lower layer sediments (extending from 10 to 12.5 cm below the streambed). The hydraulic conductivity (K) of the upper bed sediments and the lower bed sediments was measured in situ. Several locations within the streambed exhibited an increase in tracer concentration with depth, suggesting the presence of horizontal flow paths within this small pool. Over the entire pool, the influence of K heterogeneity on hyporheic exchange was masked by the groundwater head gradient and the morphology of the stream. Together, the groundwater head gradient and stream morphology induced a generally high tracer concentration and fast hyporheic exchange on the left side and center of the channel and low concentrations and slower exchange on the right side. Although the reach-scale effects on the surface water concentration were small, groundwater greatly influenced the local-scale hyporheic exchange in the pool. Understanding how physical stream characteristics control the location and extent of hyporheic exchange pathways will lead to a better understanding of biogeochemical cycling of nutrients and contaminants.

Introduction

The hyporheic zone has been shown to play an important role in the chemical and biological functions of streams. Dissolved oxygen (DO) decreases rapidly with distance from the stream channel (*1*), and ammonia typically increases with distance from channel (*1–3*). Dissolved organic carbon is metabolized within the hyporheic zone (*4*), and nitrate-nitrogen is removed through dentrification (*5*) in low DO regions of the hyporheic zone. Phosphorus uptake tends to increase as the size of the hyporheic zone increases (*6*, *7*). The hyporheic zone size and exchange rate have also been shown to influence gross primary productivity, community respiration, and community metabolism (*5*, *6*, *8*, *9*). Knowing that hyporheic exchange plays an important role in ecosystem function, including nutrient cycling and community metabolism, it becomes important to understand those physical stream characteristics that influence hyporheic exchange.

Hyporheic exchange flow has been shown to be affected by stream morphology (*10*), bathymetry (*11–13*), head gradient (*14*), and mean hydraulic conductivity, K (*15*). More recent work has shown that hyporheic exchange can be dominated by K heterogeneity when the pressure head variation (e.g., due to bed forms) is small (*16*). In addition, K heterogeneity can induce a shallower hyporheic zone with a higher exchange rate (*17*) and increases in the vertical variation in K can result in increases in the mass of tracer observed in the hyporheic zone (*18*).

Of the studies that examined the role of K heterogeneity, only Ryan and Boufadel (*18*) was a field-based study. However, that study suffered from a limited data set (six hyporheic sampling locations and 85 K measurements over an 80 m reach). The current study focuses on a single 15 m long pool located at the upstream end of the reach studied by Ryan and Boufadel (*18*). A conservative tracer injection experiment was conducted, and within this pool, the hyporheic zone was monitored at 30 locations and K was measured at 119 locations in each of two bed sediment layers. The physical location, extent, and exchange rate of the hyporheic zone within this pool were evaluated in light of the measured K values and other physical characteristics.

Site Description. Indian Creek is located within the Piedmont physiographic region, and the streambed is primarily gravel and cobble sediment whose pore spaces are filled with significant amounts of sand and silt. The stream begins in the urbanized southwest part of Montgomery County in southeast Pennsylvania. Impervious surface coverage in the upper portion of the watershed is as high as 50%, and the channel is often constrained by concrete or stone walls. Proceeding in a generally southerly direction, the stream enters the western edge of the City of Philadelphia, where it is protected as part of the city's Fairmount Park system. At this point, the riparian corridor widens to as much as 200 m and consists of a deciduous forest on steep valley sides (20–25% slope). A combined sewer system (carrying sanitary sewage and stormwater during rain events) parallels both sides of the stream. One combined sewer outfall (which discharges only during large rain events) was located within the study reach.

Two surface water monitoring stations, used in previous tracer injection experiments (*18*, *19*), were established (Figure 1). The first station (S1) was located at a riffle 138 m downstream of the injection point. The second station (S2) was located 246 m downstream of the injection point (108 m downstream of S1). Between these two stations, the stream consists of three pools separated by two riffles.

The first pool was 15 m long, 4 m wide, and as much as 0.6 m deep. A large gravel bar (15 m long × 13 m wide) was located to the right of this pool. All hyporheic samples and hydraulic conductivity measurements were made within this pool. The second pool was 25 m long, 8 m wide, and 0.8 m deep at its deepest point. A combined-sewer outfall enters the stream at this location. The third pool was 19 m long, 6 m wide, and 0.3 m deep at its deepest point. Downstream of the third pool was a riffle-pool/step-pool transition zone. S2 was located at the downstream end of this transition zone.

Materials and Methods

The stream channel and portions of the floodplains along the 246 m reach were surveyed on an approximate 1 m × 1

* Corresponding author phone: (215)204-7871; fax: (215)204-4696; e-mail: boufadel@temple.edu.

10.1021/es061603z CCC: $37.00

Published on Web 05/10/2007

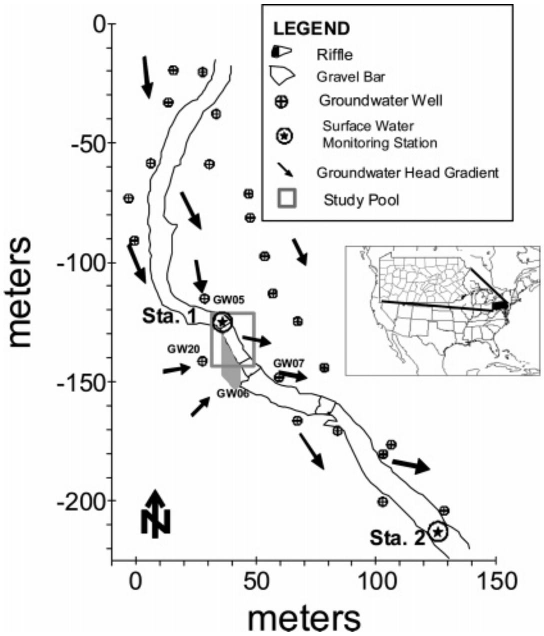

FIGURE 1. Location map of Indian Creek showing surface water monitoring stations and groundwater monitoring wells. Only select wells are labeled for clarity. The instrumented pool is located within the heavy gray box.

m grid using a TOPCON model 212D Total Station with a published angular accuracy of 6 s. The datum (i.e., zero elevation) was arbitrarily selected near the injection point. The survey occurred over 3 days during January 2006, about 2 months after the tracer study. There were no large storms or extreme flow events that would have significantly altered the channel morphology between the stream tracer study and the survey.

A conservative tracer (NaBr) injection experiment was conducted November 5−7, 2005. The injection began at noon on day 1 ($t = 0$) and continued for 22.5 h. The measured injectate concentration was 76.27 g L^{-1} Br^{-}. The injection rate averaged 9.3 mL s^{-1} using a Masterflex L/S 12VDC pump (model 7533−-40) with an EasyLoad 3 pump head (Masterflex model 77800−-52). The stream discharge was measured approximately 15 m downstream of the injection point using a Pygmy meter connected to an AQUACalc 5000 handheld computer according to standard USGS methods (*19*).

Surface water samples at S1 and S2 were collected for 36 h after the start of the injection. Samples were obtained every 3 min during the rising and falling limb of the breakthrough curve (BTC) and hourly during the plateau portion of the BTC. All surface water samples were collected from the center of the cross-sections using ISCO model 3700 autosamplers.

The hyporheic zone was sampled for approximately 48 h after the start of injection. Thirty hyporheic sampling ports were installed in the first pool downstream of S1. Port locations are shown as filled triangles in Figure 2. The location of each port was determined through triangulation with previously established benchmarks. The locations of the benchmarks were confirmed during the January 2006 survey. Each hyporheic port was sampled up to 10 times beginning at $t = 0$ h (the start of injection) and continuing during daylight hours until approximately $t = 48$ h (24.5 h after the injection ended).

Each port was made of 1.5 cm i.d. iron pipe that was capped on one end and perforated with 3.2 mm holes over a 2.5 cm segment. Three pairs of ports were pounded into the streambed along each of five transects. One port of each pair was installed such that the perforations extended from

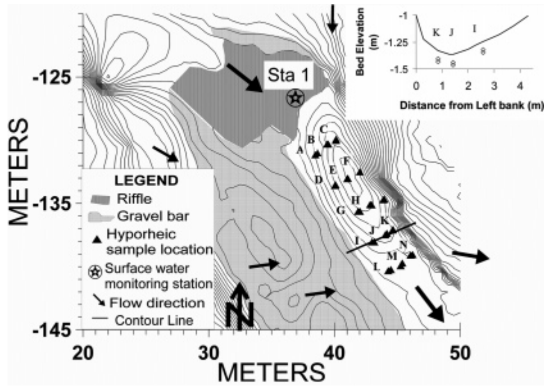

FIGURE 2. Bathymetric map of study pool with inset showing cross-section and subsurface sample locations for transect K−J−I. Bathymetric contour interval is 10 cm. Hyporheic sampling location labels correspond to labels in Figure 4. Groundwater flow was generally down valley. However, note that the flow across the large gravel bar along the right bank was almost perpendicular to the stream flow. This head gradient would minimize subsurface influx along the right side of the channel and maximize subsurface influx along the center and left side of the channel.

7.5 to 10 cm below the streambed (upper sediment layer), and one port was installed such that the perforations extended from 10 to 12.5 cm below the streambed (lower sediment layer). The ports making up each pair were placed on average 13 cm apart. Each pair was approximately 0.9 m apart, and each transect was approximately 2.8 m apart. Each port was outfitted with 0.32 cm i.d. vinyl tubing that extended from near the bottom of the port to the stream bank and was labeled with a unique port identification code. Samples were collected using a Masterflex L/S 12VDC pump (model 7533-20), cartridge pump head (model 07519-80), and eight small cartridges (model 7519-80), each loaded with a length of 0.16 cm diameter C-Flex tubing. For each sampling event, eight ports were connected to the pump system, and the first 200 mL of sample was wasted to clear the port and tubing of old water. The sample cups were then rinsed for 1 min, and finally a sample was collected in the rinsed cup. This procedure was repeated until all 30 ports were sampled.

All surface water and hyporheic samples were analyzed using a Dionex 500 ion chromatograph. One out of every 10 samples was run in duplicate (CV = 0.035). The injectate samples were diluted by a factor of 10^5 prior to analysis. The injectate samples were also analyzed (without dilution) using an Orion IonAnalyzer model 407A meter with a Mettler Toledo bromide ISE and a Cole-Parmer single junction reference electrode. The results of both methods were in agreement.

The hydraulic conductivity of the streambed within the first pool downstream of S1 was measured in situ using a small diameter, portable, falling head permeameter (*18*, *20*, *21*) in a period of 2 weeks following the tracer experiment. The permeameter consisted of a PVC reservoir threaded to a ball valve, which was threaded to a hollow steel pipe. The steel pipe had an inside diameter of 1.2 cm and outside diameter of 2.2 cm. A solid steel drive point was attached to the bottom of the pipe. Beginning a few millimeters above the bottom, the pipe was evenly perforated over a 2.5 cm section with 12 holes each 0.9 cm in diameter. The perforated section was wrapped with stainless steel mesh having an opening size of 178 μm. The pipe was clearly marked at 7.5 and 10 cm above the top of the perforations.

At each K measurement location, the pipe, without the reservoir and ball valve, was inserted or pounded into the streambed such that the top of the perforations was 7.5 cm below the bed surface. The reservoir and ball valve were attached to the pipe, and the reservoir was filled with streamwater while the ball valve was closed. The ball valve

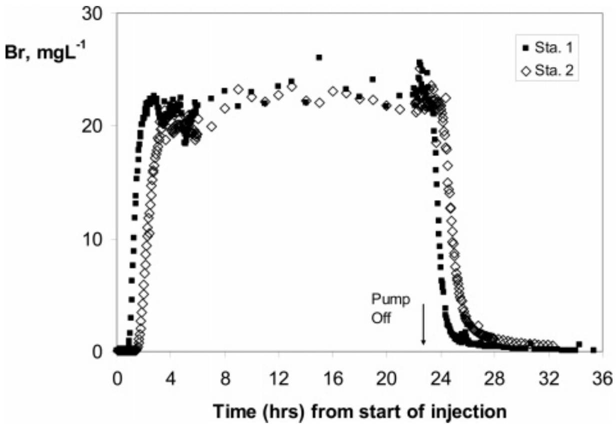

FIGURE 3. Breakthrough curves for surface water monitoring S1 and S2. Injection was continuous for 22.5 h. The plateau concentration at S2 was statistically lower than that of S1 (Wilcoxon−Mann−Whitney Rank Sum Test, $p = 0.001$).

was then opened instantly, causing a decrease in the water level in the reservoir. The water level in the reservoir was recorded at predetermined timed intervals. The test was run until the reservoir emptied or 20 min had passed. After the test was completed, the reservoir and ball valve were removed, and the permeameter pipe was driven an additional 2.5 cm into the bed sediment so that the top of the perforations was 10 cm below the bed surface. The reservoir/ball valve assembly was replaced, and the test was repeated. In this way, the upper sediment layer (7.5−10 cm below the streambed) and lower sediment layer (10−12.5 cm below the streambed) measurements were made in the same location and thus constitute paired samples. A total of 238 *K* measurements was obtained at 119 locations on 15 transects. The test results were interpreted using the method of Hvorslev (ref *22*, Figure 18G).

It has long been recognized that *K* influences surface−subsurface exchange (*23*, *24*). If one defines exchange as the rate at which surface water enters or exits the hyporheic zone, then exchange can be quantified by the slope of the rising or falling limb of the hyporheic BTC, and this exchange can be correlated with the variation in hydraulic conductivity. The values of *K* and ln *K* at each hyporheic port location were estimated from the measured data. In addition, the variance of *K* (σ^2_K) and variance of ln *K* ($\sigma^2_{\ln K}$) were estimated for each port based on the *K* values measured within 2 m upstream and 1 m downstream of each port. Each of these four parameters was correlated with the slope of the initial rising limb (first 2−3 h of the BTC) and late falling limb (last 20−22 h of BTC) of the hyporheic breakthrough curves. The slope of the initial rising limb of the BTC was estimated assuming a linear relationship, and the slope of the late falling limb of the BTC was estimated assuming a power law relationship. The analysis was done for each channel location (left side, right side, and center of channel) and for each sediment layer (upper and lower layer) as well as for the combined data sets. Groundwater elevation near the stream was determined from 24 bankside groundwater monitoring wells (Figure 1).

Results

The streamflow rate averaged 13.2 L s^{-1} near the injection point. BTCs for each of the surface water monitoring stations are shown in Figure 3. The average plateau Br^- concentration was 21.8 and 21.1 mg L^{-1} at S1 and S2, respectively. The small reduction in tracer concentration was statistically significant (Wilcoxon−Mann−Whitney Rank Sum Test, $p = 0.001$) and is attributable to groundwater dilution. The bromide concentration at S1 returned to background levels (<0.1 mg L^{-1}) by $t = 33$ h (10.5 h after the injection ended). At S2, sampling ended at $t = 32.33$ h (i.e., 9.83 h after the injection ended) due to autosampler failure. The instream Br^- concentration was approximately 0.5 mg L^{-1} at that time.

Surface water elevation in the pool was at −1.0 m (arbitrary survey datum). Groundwater elevations on the left bank ranged from −0.7 m at groundwater well #5 (GW#5) to −1.19 m at GW#7. On the right bank, the groundwater elevation was −0.86 m at GW#20 and −0.95 m at GW#6. The hydraulic gradient at the large scale was generally in the down valley direction (Figure 1), while the local-scale gradient was from the right bank toward the left bank of the pool outlet (Figure 2).

The *K* values measured in the upper layer ranged from 1.71×10^{-4} to 1.80×10^{-1} cm s^{-1}, with a mean value of 1.99×10^{-2} cm s^{-1}. This layer was relatively heterogeneous with a variance of the logarithmically transformed data ($\sigma^2_{\ln K}$) equal to 2.0. The *K* values measured in the lower layer ranged from 1.81×10^{-4} to 1.34×10^{-1} cm s^{-1} with an average value of 1.66×10^{-2} cm s^{-1} and $\sigma^2_{\ln K} = 1.71$. The measured *K* values were consistent with previously published data for this stream (*18*).

The two sediment layers had no significant difference in mean ln *K* (Student's *t* test, $p > 0.1$) or in $\sigma^2_{\ln K}$ (*F* test, $p > 0.1$). However, significant differences in mean ln *K* were found when the dataset was broken out by channel location (left, center, and right side of stream). The left side (i.e., the outer side of the meander) had significantly smaller ln *K* values than the right side as a whole ($p = 0.007$), within just the upper layer ($p = 0.07$) and within just the lower layer ($p = 0.05$). The left side also had significantly smaller ln *K* values than the center of the channel as a whole ($p = 0.06$), although there was no significant difference in ln *K* values within the individual sediment layers.

It has been shown by past studies that hyporheic exchange and hydraulic conductivity are positively related (*15*, *18*, *25*, *26*). Thus, the variation in ln *K* observed in Indian Creek suggests that the percent of surface water observed in the hyporheic zone should be lower along the left side of the channel and higher along the right side of the channel. However, this was not the case as is discussed next.

BTCs in the hyporheic zone are shown in Figure 4 for 25 ports. The remaining five ports are not shown because they were dry throughout the sampling events, most likely due to clogging during installation. The Wilcoxon−Mann−Whitney Rank Sum Test was used to analyze the maximum hyporheic tracer concentrations in the ports. The maximum concentrations observed along the right side of the channel were significantly lower than the concentrations observed along the left side of the channel in the upper sediment layer ($p = 0.03$), lower sediment layer ($p = 0.03$), and in both layers combined ($p = 0.001$). Similarly, the maximum observed concentrations observed along the right side were lower than the concentrations observed in the center of the channel in the upper sediment layer ($p = 0.03$), lower sediment layer ($p = 0.06$), and in both layers combined ($p = 0.0005$).

Hyporheic loading and flushing can be assessed by examining the change in concentration of the tracer with respect to time. In both sediment layers, hyporheic loading is greatest along the left side near the pool entrance, where the hyporheic tracer concentrations were near 20 mg L^{-1} (90% surface water) within 4 h (Figure 4C,F). Hyporheic flushing also occurred rapidly in this area of the streambed. At $t = 25.5$ h (3 h after the injection was stopped), the hyporheic concentration was 5.1 mg L^{-1} in the upper layer and 3.0 mg L^{-1} in the lower layer. In contrast, the hyporheic zone along the right side near the pool inlet was loaded and flushed at a much slower rate. At $t = 4$ h, the hyporheic concentration in the upper sediment layer along the right side at the pool inlet (Figure 4A) was approximately 12.7 mg

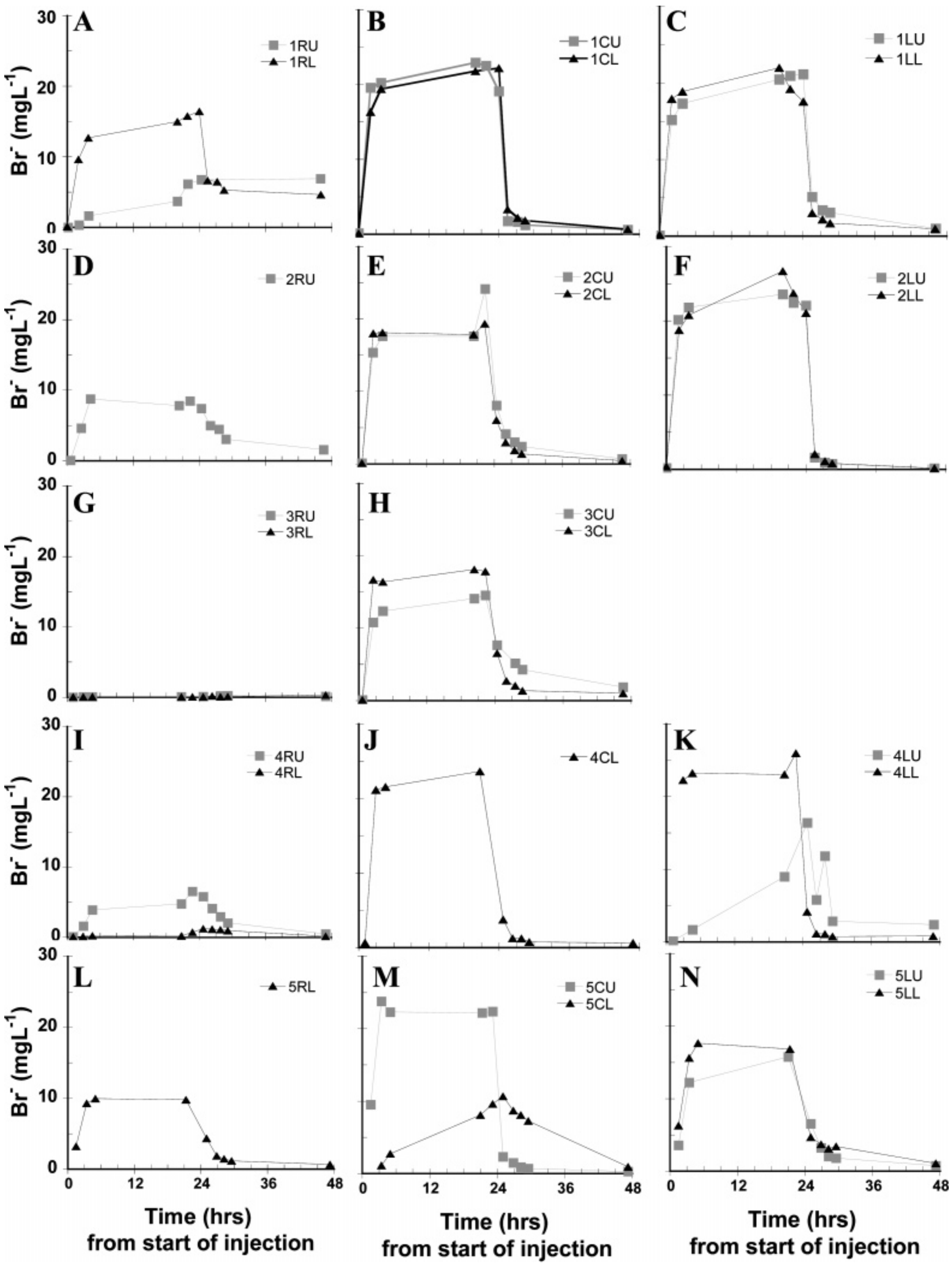

FIGURE 4. Breakthrough curves for the hyporheic sampling ports. Slides are arranged from upstream (top of figure) to downstream (bottom of figure). Ports are identified by the transect number (1: upstream to 5: downstream), location within transect (L: left, C: center, and R: right as viewed looking downstream), and sediment layer (U: upper sediment layer and L: lower sediment layer). Results from ports that were dry (likely due to clogging of the port screen) are not shown. The maximum tracer concentration in the lower sediment layer exceeded that of the upper sediment layer along a pathway extending from the right side at the pool inlet (A), through the center of the pool (H), to the left side at the pool outlet (K and N). This phenomenon is indicative of horizontal hyporheic flux in this pool.

L^{-1} or 58% surface water, while in the lower sediment layer, the concentration at this time was just 1.7 mg L^{-1} or less than 8% surface water. At $t = 46.5$ h (24 h after the injection was ended), the hyporheic concentration at this location was still more than 6.9 mg L^{-1} in the upper layer and more than 4.6 mg L^{-1} in the lower layer (Figure 4A). The mid-pool right side had the least hyporheic exchange with concentrations never exceeding 9 mg L^{-1} in the upper sediment layer (Figure 4D) or 2 mg L^{-1} in the lower sediment layer (Figure 4I).

Hyporheic loading and flushing tended to be faster in the lower sediment layer than in the upper sediment layer. From the time of initial loading through the time of maximum observed hyporheic tracer concentration, the areas of high tracer concentration were more extensive in the lower sediment layer. For example, at $t = 23$ h, the area of the lower sediment layer with concentrations greater than 20 mg L^{-1} included the left side of the channel from the inlet to near the outlet (Figure 4C,F,K) as well as the center of the channel at the pool inlet and near the mid-pool area (Figure 4B,J). In the upper sediment layer, the area with concentrations greater than 20 mg L^{-1} was limited to the left side of the pool inlet (Figure 4C) and center of the pool outlet (Figure 4M).

During the flushing stages, the areas of high concentration were more extensive in the upper sediment layer. At $t =$ 25 h, the tracer concentration in the upper sediment layer was more than 1 mg L^{-1} greater than that of the lower layer along the left side of the channel at the pool inlet (Figure 4C) and outlet (Figure 4K,N), in the center of the channel at mid-pool (Figure 4E,G), and on the right side of the channel near the pool outlet (Figure 4I). Only in the center of the channel at the pool inlet (Figure 4B) and outlet (Figure 4M) was the lower layer sediment concentration more than 1 mg L^{-1} greater than the upper layer sediment.

At $t = 46.5$ h, the tracer concentration in the upper sediment layer was greater than that of the lower sediment layer along a flow path that extended from the right side of the pool inlet (Figure 4A) through the center of the channel at mid-pool (Figure 4E,H) toward the left side of the channel near the pool outlet (Figure 4K). In fact, at $t = 46.5$ h, the tracer concentration throughout the entire lower layer, with the exception of the right side pool inlet, was approximately 1.0 mg L^{-1} or less, while the concentration in the upper layer was approximately 2.0 mg L^{-1} or more at three locations.

While it has long been recognized that K influences surface−subsurface exchange (*23*, *24*), a strong relationship was not found between hydraulic conductivity and surface−subsurface exchange in this pool of Indian Creek. The highest correlation coefficients were found between K and the slope of the late falling limb of the BTC ($|R| = 0.31-0.67$). Except along the left side of the channel where $R = -0.31$, all correlations were positive, suggesting that exchange increases with K. Along the left side of the channel, it is likely that other factors such as the groundwater head gradient and channel morphology have a greater influence on exchange than does K. The negative relationship is counterintuitive and requires further research.

The influence of hydraulic conductivity heterogeneity (as defined by σ^2_K and $\sigma^2_{\ln K}$) also appears to be small in this pool. The correlation coefficients with σ^2_K accounted for only 18−53% of the variation in the slope of the late falling limb of the BTC. The correlation coefficients with $\sigma^2_{\ln K}$ accounted for only 2−41% of this same variation.

Discussion

Hyporheic exchange is an important component to the biochemical processes of stream ecosystems. In one study of a California mountain stream (*1*), nitrification caused the NH_4 concentration to decrease and NO_3 concentration to increase as groundwater with a high NH_4 concentration approached the oxygenated surface waters. The NO_3 concentration reached a peak within the hyporheic zone and then decreased toward the surface water, likely due to biological uptake. In another study (*4*), microbial activity caused the dissolved organic carbon and dissolved oxygen to decrease and dissolved inorganic carbon to increase along hyporheic flow paths. In Appalachian mountain streams, phosphorus uptake was found to increase with hyporheic exchange (*6*). In a study of a desert stream (*5*), hyporheic respiration was found to be a significant portion of total stream respiration. The inclusion of hyporheic processes in the whole stream metabolism calculation yielded results that suggested that the stream was heterotrophic while the exclusion of hyporheic processes yielded results that suggested that the stream was autotrophic. A significant relationship between whole stream metabolism and hyporheic exchange was also found in mountain streams of the southwest U.S. (*8*). In one of the few studies of hyporheic processes of large rivers (*27*), it was found that the hyporheic zone of the mid-channel of the Elbe River, Germany provided greater microbial uptake than the hyporheic zone along the channel edges due to greater exchange rates caused by looser mid-channel sediments. In urban streams such as Indian Creek, the location and physical extent of these pathways may be especially important in processing excess nutrients, bacteria, and other contaminants associated with both urban stormwater runoff and combined sewer outfalls.

Subsurface tracer flux can occur in the vertical or horizontal direction. During the plateau portion of an injection experiment, the surface water concentration will always be equal to or greater than the hyporheic concentration. Thus, when vertical surface−subsurface exchange is dominant, one would expect the tracer concentration to decrease (or remain relatively constant) with depth in the bed sediment. However, when the tracer concentration increases with depth, horizontal flux must be dominant at that location. This phenomenon could occur when vertical flux carries the tracer into deeper areas of the hyporheic zone and then horizontal flux carries the tracer into areas with low vertical flux.

As shown in Figure 4, horizontal flux appears to dominate hyporheic exchange in an area that extends roughly from the right side of the streambed at the pool entrance through the center of the channel to the left side of the streambed at the pool exit. This is the first time such a pathway for hyporheic exchange is speculated in field studies. In other locations within the pool, particularly the left and center of the channel near the pool inlet and the center of the channel near the pool outlet, the hyporheic tracer concentration is high (>50% of the surface water concentration), and the tracer concentration in the upper sediment layer is as high as or higher than that observed in the lower sediment layer. In these areas, vertical exchange flux may be important as well. In a third area of the stream (along the right side of the channel), very little tracer was observed in either sediment layer.

The differences in observed hyporheic tracer concentration across the channel are likely due to a combination of variables including the sediment hydraulic conductivity, stream morphology, bathymetry, and head gradient. Recognizing that K influences surface−subsurface exchange (*23*, *24*), and defining exchange as the rate at which surface water enters or exits the hyporheic zone, it would seem intuitive that the slopes of the rising and falling limbs of the BTC are likely to be influenced by K. In the pool of Indian Creek studied herein, however, a strong relationship between hydraulic conductivity and exchange was not found.

More recently, researchers have begun to examine the role that streambed heterogeneity plays in surface−subsurface exchange (*16*−*18*). As with hydraulic conductivity, the influence of heterogeneity (as defined by σ^2_K and $\sigma^2_{\ln K}$) also appears to be small in this pool. While not statistically significant, it is interesting to note that heterogeneity had a negative influence on the slope of the late falling limb of the BTC. Thus, in contrast to the findings of Salehin et al. (*17*), as the variance of K increased in this small pool, the exchange rate decreased.

Hyporheic exchange has been shown to be related to stream morphology and bathymetry (*11*−*13*, *16*). These studies suggest that exchange will be greater in areas with increased velocity and pressure heads. The stream morphology and bathymetry of Indian Creek in the vicinity of the instrumented pool are shown in Figures 1 and 2. From an examination of these two figures, it is clear that the stream flow is directed toward the left side of the channel at the pool inlet. This suggests that flow velocities and pressure heads, and thus exchange, would be greater along the left side of the channel than along the right.

On the basis of elevation measurements in the 24 bankside wells, the groundwater head gradient was generally down valley. However, within the instrumented pool, the bankside monitoring wells suggested that the head gradient may have been much more sharply from the right side toward the left side as shown in Figure 2. In addition, with the exception of the upper sediment at the pool inlet, the right side hyporheic concentrations were no more than 45% of the surface water plateau concentrations (Figure 4A,D,G,I,L) and thus at least 55% groundwater. Along the left side of the pool (Figure 4C,F,K,N), the hyporheic concentrations were at least 75% surface water (or less than 25% groundwater). In contrast, the stream flow increased by only 3% within the 108 m reach bounded by surface water monitoring S1 and S2. So while groundwater had a minimal effect on surface water concentrations, its influence on the hyporheic zone was strong, especially in the mid-pool region.

In a prior study, Ryan and Boufadel (*18*) demonstrated the importance of hydraulic conductivity heterogeneity in controlling hyporheic exchange over an 80 m reach of Indian Creek. At that larger scale, and perhaps due to the placement of ports in areas with similar groundwater head gradients, vertical heterogeneity was shown to be an important factor in controlling hyporheic exchange. In the current study, 25 ports were sampled in just the first pool of the previous study. However, at the scale of the single pool studied herein, the influence of morphology, and possibly groundwater head gradient, may have masked the influence of *K*. A detailed model incorporating *K*, morphology, and head gradient is needed to discern the influence of the multiple forces driving hyporheic exchange.

Knowing the approximate locations for areas of vertical or horizontal flux domination gives a starting point for determining biogeochemical transformations along otherwise unknown pathways. While many researchers have identified the upstream and downstream sides of riffles and other geomorphic features as downwelling and upwelling zones (*10*−*13*), the research herein demonstrates that downwelling and upwelling can occur within the pools between riffles. These areas must also be investigated as potential hotspots of biogeochemical processing.

Acknowledgments

We gratefully acknowledge the assistance of the Fairmount Park Commission and the Overbrook Farms Beautification Committee. We also gratefully acknowledge the assistance of Sandeep Argarwal, Kevin Yao, Peter Lokken, Abdullah Fall, Qinghong Zhao, and Liang Luo for their help with the field work. Funding for this work was provided by the U.S. Department of Agriculture, Grant PENR-2003-01280. However, no official endorsement should be inferred.

Literature Cited

(1) Triska, F. J.; Kennedy, V. C.; Avanzino, R. J.; Zellweger, G. W.; Bencala, K. E. Retention and transport of nutrients in a third-order stream in northwestern California: Hyporheic processes. *Ecology* **1989**, *70*, 1893−1905.

(2) Triska, F. J.; Duff, J. H.; Avanzino, R. J. Patterns of hydrological exchange and nutrient transformation in the hyporheic zone of a gravel-bottom stream: Examining terrestrial−aquatic linkages. *Freshwater Biol.* **1993**, *29*, 259−274.

(3) Hill, A. R.; Labadia, C. F.; Sanmugadas, K. Hyporheic zone hydrology and nitrogen dynamics in relation to the streambed topography of a N-rich stream. *Biogeochemistry* **1998**, *42*, 285−310.

(4) Findlay, S.; Strayer, D.; Goumbala, C.; Gould, K. Metabolism of streamwater dissolved organic carbon in the shallow hyporheic zone. *Limnol. Oceanogr.* **1993**, *38*, 1493−1499.

(5) Grimm, N. B.; Fisher, S. G. Exchange between interstitial and surface water: Implications for stream metabolism and nutrient cycling. *Hydrobiologia* **1984**, *111*, 219−228.

(6) Mulholland, P. J.; Marzolf, E. R.; Webster, J. R.; Hart, D. R.; Hendricks, S. P. Evidence that hyporheic zones increase heterotrophic metabolism and phosphorus uptake in forest streams. *Limnol. Oceanogr.* **1997**, *42*, 443−451.

(7) Hall, R. O.; Bernhardt, E. S.; Likens, G. E. Relating nutrient uptake with transient storage in forested mountain streams. *Limnol. Oceanogr.* **2002**, *47*, 255−265.

(8) Fellows, C. S.; Valett, H. M.; Dahm, C. D. Whole-stream metabolism in two montane streams: Contribution of the hyporheic zone. *Limnol. Oceanogr.* **2001**, *46*, 523−531.

(9) Mulholland, P. J.; Fellows, C. S.; Tank, J. L.; Grimm, N. B.; Webster, J. R.; Hamilton, S. K.; Marti, E.; Ashkenas, L.; Bowden, W. B.; Dodds, W. K.; McDowell, W. H.; Paul, M. J.; Peterson, B. J. Interbiome comparison of factors controlling stream metabolism. *Freshwater Biol.* **2001**, *46*, 1503−1517.

(10) Kasahara, T.; Wondzell, S. M. Geomorphic controls on hyporheic exchange flow in mountain streams. *Water Resour. Res.* **2003**, *39*, 1005, doi:10.1029/2002WR001386.

(11) Elliott, A. H.; Brooks, N. H. Transfer of nonsorbing solutes to a streambed with bed forms: Theory. *Water Resour. Res.* **1997**, *33*, 123−136.

(12) Elliott, A. H.; Brooks, N. H. Transfer of nonsorbing solutes to a streambed with bed forms: Laboratory experiments. *Water Resour. Res.* **1997**, *33*, 137−151.

(13) Harvey, J. W.; Bencala, K. E. The effect of streambed topography on surface−subsurface water exchange in mountain catchments. *Water Resour. Res.* **1993**, *29*, 89−98.

(14) Morrice, J. A.; Valett, H. M.; Dahm, C. D.; Campana, M. E. Alluvial characteristics, groundwater−surface water exchange, and hydrological retention in headwater streams. *Hydrol. Proc.* **1997**, *11*, 253−267.

(15) Ryan, R. J.; Packman, A. I. Changes in streambed sediment characteristics and solute transport in the headwaters of Valley Creek, an urbanizing watershed. *J. Hydrol.* **2006**, *323*, 74−91.

(16) Cardenas, M. B.; Wilson, J. L.; Zlotnik, V. A. Impact of heterogeneity, bed forms, and stream curvature on subchannel hyporheic exchange. *Water Resour. Res.* **2004**, *40*, W08307, doi:10.1029/2004WR003008.

(17) Salehin, M.; Packman, A. I.; Paradis, M. Hyporheic exchange with heterogeneous streambeds: Laboratory experiments and modeling. *Water Resour. Res.* **2004**, *40*, W11504, doi:10.1029/2003WR002567.

(18) Ryan, R. J.; Boufadel, M. C. Influence of streambed hydraulic conductivity on solute exchange with the hyporheic zone. *Environ. Geol.* **2006** *51*, 203−210.

(19) Carter, R. W.; Davidian, J. *General Procedures for Gauging Streams*; U.S. Geologic Survey: Reston, VA, 1968.

(20) Landon, M. K.; Rus, D. L.; Harvey, F. E. Comparison of instream methods for measuring hydraulic conductivity in sandy streambeds. *Ground Water* **2001**, *39*, 870−885.

(21) Freeze, R. A.; Cherry, J. A. *Groundwater*; Prentice Hall: Englewood Cliffs, NJ, 1979.

(22) Hvorslev, M. J. *Time Lag and Soil Permeability in Groundwater Observations*; U.S. Army Corps. of Engineers, Waterways Experiment Station: Washington, DC, 1951.

(23) Vaux, W. G. Intragravel flow and interchange of water in a streambed. *Fish. Bull.* **1968**, *66*, 479−489.

(24) Savant, S. A.; Reible, D. D.; Thibodeaux, L. J. Convective transport within stable river sediments. *Water Resour. Res.* **1987**, *23*, 1763−1768.

(25) Wörman, A.; Packman, A. I.; Johansson, H.; Jonsson, K. Effect of flow-induced exchange in hyporheic zones on longitudinal transport of solutes in streams and rivers. *Water Resour. Res.* **2002**, *38*, 1001, doi:10.1029/2001WR000769.

(26) Wörman, A.; Packman, A. I.; Johansson, H.; Jonsson, K. Correction to "Effect of flow-induced exchange in hyporheic zones on longitudinal transport of solutes in streams and rivers" by Anders Wörman et al. *Water Resour. Res.* **2002**, *38*, 1070, doi:10.1029/2001WR001175.

(27) Fischer, H.; Kloep, F.; Wilzcek, S.; Pusch, M. T. A river's liver-microbial processes within the hyporheic zone of a large lowland river. *Biogeochemistry* **2005**, *76*, 349−371.

Received for review July 6, 2006. Revised manuscript received March 24, 2007. Accepted April 2, 2007.

ES061603Z